Perestroikas of strange attractors

Tsvetelin Tsankov[†], Christophe Letellier[‡], Greg Byrne[§] and Robert Gilmore[§]

[†] *Physics Department, Bryn Mawr College, Bryn Mawr, PA 19010-2899, USA*

[‡] *CORIA UMR 6614 - Université de Rouen, BP 12, Av. de l'Université, Saint-Etienne du Rouvray cedex, France*

[§] *Physics Department, Drexel University, Philadelphia, Pennsylvania 19104, USA*

(Dated: November 15, 2004, *Physical Review E*: To be submitted.)

Strange attractors can exhibit bifurcations just as periodic orbits in these attractors can exhibit bifurcations. We describe two classes of large-scale bifurcations that strange attractors can undergo. For each we provide a mechanism. These bifurcations are illustrated in a simple class of three-dimensional dynamical systems.

I. INTRODUCTION

Strange attractors are generated by dynamical systems that depend on parameters. These are deterministic sets of first order nonlinear ordinary differential equations of the form $\dot{x}_i = f_i(x;c)$, where the state variables x_i define the state of the system and the control parameters c can be varied. State variables typically model physical variables (laser intensity, concentration of chemical species) and control variables typically model experimental conditions (laser pumping rates, chemical flow rates). As the control parameters c are varied strange attractors undergo changes. It is one of the goals of dynamical systems theory to understand and predict the spectrum of changes that a nonlinear dynamical system can undergo under parameter variations [1–5].

Some changes are simple and well-known. These involve bifurcations of fixed points and of periodic orbits. Fixed point bifurcations are described by the theory of singularities [6–8]. The bifurcations that periodic orbits can undergo when a single parameter is varied include only period-doubling bifurcations and saddle-node bifurcations [1–5]. However, strange attractors themselves can undergo bifurcations as control parameters change. It is now possible to study the spectrum of bifurcations that strange attractors can undergo because of the structures that have been introduced to describe and classify strange attractors in three dimensions. As these bifurcations go beyond the bifurcations allowed to fixed points and periodic orbits, we call these new kinds of bifurcations "perestroikas," a term commonly used in catastrophe theory and the theory of singularities [6–9]. Perestroikas involve changes in the structures we use to characterize strange attactors. These are knot holders [10, 11, 4, 5], which describe how the periodic orbits in a strange attractor are organized, and bounding tori [12, 13], which describe how the knot-holders themselves are organized.

This paper is organized as follows. In Sec. II we review some of the tools that are important for the description of the global changes that strange attractors can undergo under parameter variation. In Sec. III we describe a known perestroika that occurs in the Rössler equations. We also introduce the ideas necessary to describe even larger-scale perestroikas. In Sec. IV we introduce a restricted class of familiar dynamical systems which exhibits this larger type of perestroika. In the following section we describe the mechanism that is involved in this class of perestroikas, and show in detail how the mechanism occurs in the simple class of dynamical systems introduced in Sec. IV. In Sec. VI we discuss another related mechanism giving rise to large scale changes in the structure of strange attractors. This example occurs for the Lorenz attractor in a certain range of control parameter values.

II. BACKGROUND

The properties of strange attractors are largely determined by the spectrum of unstable periodic orbits in the attractor and the topological organization of these orbits [1, 3–5]. The organization is completely summarized by knot holders. They are called knot holders because they hold all the (unstable) periodic orbits in the strange attractor and describe the organization of these orbits [10, 11, 4, 5]. Knot holders are also called branched manifolds. The knot holders themselves are highly constrained in the bifurcations they can undergo by bounding tori that enclose them. We briefly review the properties of branched manifolds and bounding tori.

A Branched Manifolds

Birman and Williams showed that it is possible to project a strange attractor that is contained in R^3 onto a two-dimensional structure called a branched manifold [10, 11]. This is done by projecting the flow down along

the stable direction onto a surface defined by the expanding and the flow directions. This is made rigorous by identifying all points in the flow with the same future:

$$x \sim y \text{ if } |x(t) - y(t)| \stackrel{t\to\infty}{\longrightarrow} 0$$

In this projection periodic orbits are neither created nor destroyed. Further, their topological organization remains unchanged since no self-intersections occur during this projection. As a result, the branched manifold can be used to identify the topological organization of all the unstable periodic orbits in the strange attractor. Since the unstable periodic orbits and their topological organization identify the strange attractor, this means that branched manifolds can be used to identify and classify strange attractors [14–16].

B Bounding Tori

Strange attractors and the branched manifolds that classify them can in turn be classified by their connectivity properties [12, 13]. The easiest way to do this is to "blow up" or "inflate" the semiflow on the branched manifold to a flow in a neighborhood of the branched manifold that has the appropriate limiting properties. This bounded open set (inertial manifold) in R^3 has a bounding surface. The surface is orientable: the inside contains the attractor. It is trapping: any orbit that passes through from outside to inside remains trapped inside forever. The surface is also bounded and closed. It is therefore a torus. All tori are identified by a single nonnegative integer, the topological index called the genus, g, which is the number of holes in the boundary. The surface with $g = 0$ is called a sphere and that with $g = 1$ is commonly called a torus. The blow-up of the flow induces a flow on this boundary. Although the flow on the branched manifold has no fixed points in the open neighborhood of the branched manifold, when restricted to the surface there are fixed point singularities. All are saddles. As a result, the number of fixed points is related to the genus, and this number is $2(g-1)$ [13].

The flow, restricted to the bounding torus surface, can be put into canonical form. For genus $g = 0, 1, 2, 3, 4, 5, 6, 7, 8, \ldots$ there are $0, 1, 0, 1, 1, 2, 2, 5, 6, \ldots$ inequivalent canonical forms [13]. These forms can be uniquely identified by a symbol sequence ("periodic orbit") of period $g - 1$. The number of canonical forms increases exponentially with an entropy of $\log(3)$ [17]. The canonical form for $g = 3$ is shown in Fig. 1.

C Global Poincaré Surface of Section

In three dimensions a Poincaré surface of section is a minimal two-dimensional surface with the property that all points in the attractor intersect this surface transversally an infinite number of times under the flow. The

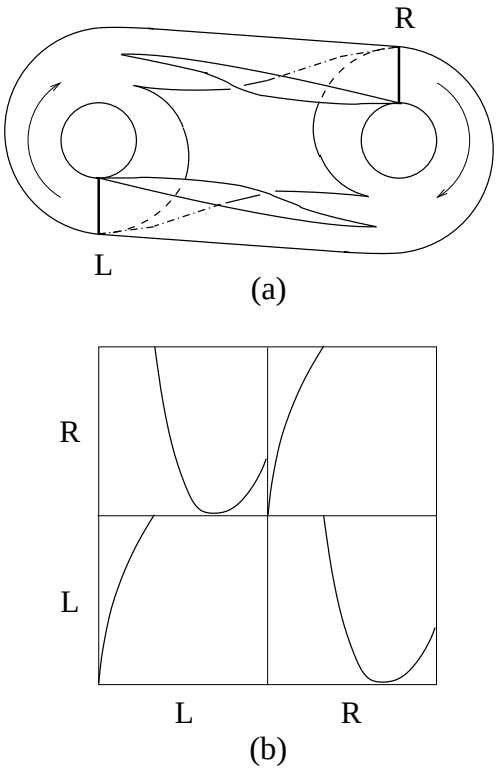

FIG. 1: Canonical form for the genus-3 bounding torus consists of an outer disk boundary and three interior holes. The four singularities are confined to the central interior hole. Locations of the two disks (L, R) comprising the Poincaré surface of section are shown.

Poincaré surface of section need not be connected and in fact is often not connected. The urge to define Poincaré sections as connected surfaces has lead to many problems in the past. The Poincaré section is generally the disjoint union of nonoverlapping disks [12, 13, 18].

The Poincaré surface for a genus-one bounding torus consists of a single disk that is transverse to the flow. The Poincaré surface for a canonical genus-g bounding torus consists of the union of $g-1$ disjoint disks. The locations of these disks are determined algorithmically [13]. The locations of the two disks for the genus-3 canonical form is shown in Fig. 1. They are labeled L and R.

D Branch Lines

Many different branched manifolds can be described by the same genus-g canonical form. Each branch line in any of these branched manifolds can be moved so that it is contained in one of the $g-1$ components of the global Poincaré surface of section. As a result, any branched manifold enclosed by a genus-g bounding torus has exactly $g-1$ branch lines.

E Return Maps

Return maps for branched manifolds enclosed by a genus-one bounding torus are well known. They are equivalent to maps from the single branch line that exists in the single component of the Poincaré section back to itself. That is, in this case return maps are exactly maps of the interval to itself. Simple continuity requirements ensure that all critical points are differentiable.

In the genus $g \geq 3$ case return maps can be constructed algorithmically [19]. There are $g-1$ branch lines. Initial conditions on any branch line flow to exactly two other branch lines. The return map is constructed as follows. Each branch line is represented as an interval. These are laid out along a horizontal axis (initial conditions). Each branch line can be oriented, from the interior to the exterior of the projection of the bounding torus onto a plane (cf., Fig. 1). As in the genus-one case, the images are arranged along the vertical axis. Over each point on the horizontal axis (consisting of $g-1$ disjoint oriented segments) there is a unique image. Each branch line has images in exactly two branch lines. Some return maps of this type are shown in Fig. 2(b) and Fig. 3(b).

F Folding and Tearing

Return maps of a branch line onto itself in a genus-one bounding torus exhibit differentiable maxima and minima that reflect the folding that takes place between adjacent branches. In bounding tori with $g \geq 3$ initial conditions on any branch line flow to exactly two other branch lines. There is some point p along each branch line with the property that initial conditions on one side evolve to one branch line and initial conditions just to the other side evolve to a different branch line. This point is called a "tearing point" and is an initial condition for the flow into a saddle type singularity. At this point the return map exhibits a jump discontinuity and often a slope discontinuity as well. These discontinuities show that tearing takes place in the flow. Tearing occurs in the neighborhood of saddle points or other singularities that deflect the flow in a small neighborhood into divergent directions [19]. Folding and tearing are exhibited in the return map shown in Fig. 2(b).

G Unfoldings of Dynamical Systems

Most of the nonlinear dynamical systems that have been studied depend on only a small number of control parameters. The Rössler and Lorenz systems depend on three control parameters. The systems presented in Sec. IV depend on one, two, or three control parameters except for the sixth system in Table 1, which depends on five. In the face of such a paucity of control parameters the full range of possible behaviors of these dynamical systems cannot be exhibited simply by varying the control parameters that are built into the model. This differs from the situation that exists in the study of catastrophes and singularities [6–9]. In these studies there is a procedure for constructing a "universal unfolding" of the singularity by adding perturbations that encapsulate all possible behaviors in a neighborhood of the singularity. There is no such theory for dynamical systems at the present time (except in the neighborhood of fixed points). Lacking such a theory, we are forced to the next best approach, which is topological in nature. In effect, we replace the (unknown) infinite dimensional universal perturbation of a dynamical system with a topological description of the system [4, 5].

III. A KNOWN PERESTROIKA

Some perestroikas are familiar and others are less so. As control parameters are changed, in the Rössler equations [20], for example, there is an alternation between chaotic and periodic behavior. The periodic behavior is seen in the form of periodic windows. In particular, as a control parameter changes a saddle node bifurcation can create a pair of periodic orbits, one of which is unstable and the other is initially stable. The stable periodic orbit "eats a hole" (window) in the bifurcation diagram, undergoes period-doubling, and eventually becomes unstable, closing the periodic window and restoring chaotic behavior. For strange attractors generated by the Smale horseshoe mechanism, the partial order in which periodic orbits can be created on the way from laminar to

chaotic behavior is constrained by topological considerations. Forcing diagrams for the simple Smale horseshoe exist to exhibit these constraints [5, 21–24].

In the perestroika just described, all the orbits can be identified by just two symbols: 0 and 1 $(a, b, c) = (?, ?, ?)$. A new class of perestroikas occurs when new orbits are created that require more than two symbols for their description using symbolic dynamics. For example, the symbol set $(0, 1)$ must be extended to $(0, 1, 2)$ to describe new orbits in the Rössler attractor in a certain range of parameter values $? < a <?$. There is an entire sequence of perestroikas in which new symbols are added (e.g., $(0, 1, 2) \rightarrow (0, 1, 2, 3)$) or removed (e.g., $(0, 1, 2, 3) \rightarrow (1, 2, 3)$) as control parameters are varied. These come about as the branched manifold that describes the strange attractor undergoes stretching and scrolling (see Figs. 7.36 and 7.45 in [5], [25]).

Sometimes even more profound changes occur as control parameters are varied. These involve changes in the global topological structure of the attractor. Such perestroikas need not involve changes in the number of symbols required to identify each periodic orbit in the attractor. In fact, what changes is the connectivity properties of the strange attractor. To be more precise, what changes is the connectivity of the branched manifold that describes the strange attractor.

IV. CLASS OF SYSTEMS STUDIED

In order to exhibit these perestroikas, it is useful to study dynamical systems that create strange attractors that can be enclosed in genus-three bounding tori. A useful collection of such strange attractors is generated by autonomous dynamical systems with a rotation $(R_Z(\pi))$ symmetry in R^3 and with forcing terms of degree not exceeding two [26]. The most general form for flows with $R_Z(\pi)$ symmetry is [27]

$$\frac{d}{dt}\begin{bmatrix} X \\ Y \\ Z \end{bmatrix} = \begin{bmatrix} F_{X,X} & F_{X,Y} & 0 \\ F_{Y,X} & F_{Y,Y} & 0 \\ 0 & 0 & F_Z \end{bmatrix} \begin{bmatrix} X \\ Y \\ 1 \end{bmatrix} \tag{1}$$

The five functions in the equation above are invariant under the actions of the group, so depend on the invariants X^2, XY, Y^2, Z. The most general dynamical system with $R_Z(\pi)$ symmetry and forcing terms of degree no higher than two is

$$\begin{aligned} \dot{X} &= a_1 X + a_2 Y + a_3 XZ + a_4 YZ \\ \dot{Y} &= b_1 X + b_2 Y + b_3 XZ + b_4 YZ \\ \dot{Z} &= c_0 + c_1 Z + c_2 X^2 + c_3 XY + c_4 Y^2 + c_5 Z^2 \end{aligned} \tag{2}$$

The values of the coefficients (a, b, c) for all the dynamical systems with these properties that have been studied are provided in Table 1.

TABLE I: Coefficients of several quadratic systems with $R_Z(\pi)$ symmetry.

System	X a_1	Y a_2	XZ a_3	YZ a_4	X b_1	Y b_2	XZ b_3	YZ b_4	- c_0	Z c_1	X^2 c_2	XY c_3	Y^2 c_4	Z^2 c_5	Ref.
1. Lorenz	$-\sigma$	$+\sigma$	0	0	R	-1	-1	0	0	$-b$	0	$+1$	0	0	[29]
2. Chen & Ueta	$-\sigma$	$+\sigma$	0	0	$R-\sigma$	R	-1	0	0	$-b$	0	$+1$	0	0	[30]
3. Wang, Singer & Bau	$-\sigma$	$+\sigma$	0	0	0	-1	-1	0	Ra	-1	0	$+1$	0	0	[31]
4. Shimizu & Morioka	0	$+1$	0	0	1	$-\mu$	-1	0	0	$-\alpha$	$+1$	0	0	0	[32]
5. Rucklidge	0	$+1$	0	0	$-\lambda$	$+\kappa$	-1	0	0	-1	$+1$	0	0	0	[33]
6. Lusseyran & Brancher	$-\alpha$	$\alpha\beta$	α	α	α	$-\alpha\gamma$	$-\alpha$	$-\alpha C$	0	$-\nu$	-1	-1	0	0	[34]
7. Burke & Shaw	$-S$	$+S$	0	0	0	-1	$-S$	0	$\mathcal{V}$	0	0	$+S$	0	0	[35]
8. Sprott B	0	0	0	$+1$	a	$-a$	0	0	b	0	-1	0	0	0	[36]
9. Sprott C	$-a$	$+a$	0	0	0	0	$+1$	0	b	0	0	-1	0	0	[36]
10. Rikitake	$-\mu$	0	0	$+1$	$-a$	$-\mu$	$+1$	0	$+1$	0	0	-1	0	0	[37]

The large scale structure of a strange attractor is largely determined by the number, location, and stability of the coexisting fixed points.

The number of fixed points is governed by Bezout's theorem [28]. This theorem states that the number of fixed points of a set of polynomial equations is bounded above by the product of the degrees of these equations. In the present case, this is $d_x \times d_y \times d_z$, where d_x is the degree of the forcing terms in the equation $\dot{X} = f(X, Y, Z)$, etc. Since we are restricting ourselves to quadratic equations

this product cannot exceed eight. In fact, for all except the sets of equations 6 and 10, this product is four.

The fixed points are of two types. They occur in symmetry-related pairs off the Z axis, and as two-fold degenerate fixed points on the Z axis. Bezout's theorem counts the number of fixed points, including their degeneracy. For all of the systems in the table above, we choose control parameter values so that there are only two off-axis fixed points that are related by the symmetry, and they are unstable foci. The remaining fixed point, if it exists, must be on the Z axis. This fixed point exists at $(0, 0, Z)$, where Z is determined by $\dot{Z} = c_0 + c_1 Z + c_5 Z^2 = 0$. Since $c_5 = 0$ for all the systems listed in the table above, the fixed point occurs at $Z = -c_0/c_1$. For the sytems 7 - 10 the fixed point is "at infinity" since $c_1 = 0$. That is, there is no fixed point. In the remaining cases (except 3) it is at 0 since $c_0 = 0$. In case 3 it occurs at $Z = \mathrm{Ra}$.

The global properties of the strange attractor are governed by the stability properties of the flow in the direction transverse to the Z axis. The stability matrix on the Z axis is

$$\begin{bmatrix} a_1 + a_3 Z & a_2 + a_4 Z & 0 \\ b_1 + b_3 Z & b_2 + b_4 Z & 0 \\ 0 & 0 & c_1 + 2c_5 Z \end{bmatrix} \tag{3}$$

From this it is clear that the eigenvectors are along and orthogonal to the symmtry axis, and the eigenvalue in the Z direction is $c_1 + 2c_5 Z$. For systems 7 - 10 the Z axis is invariant with constant nonzero flow $\dot{Z} = c_0$ along this axis.

The two other eigenvectors of the stability matrix are orthogonal to the Z axis. Their eigenvalues are determined by the 2×2 submatrix in (3). These eigenvalues determine to a large extent the global topology of the strange attractors (their genus) and the perestroikas they undergo.

TABLE II: Control parameter values for which the symmetric dynamical systems generate strange attractors that exist in genus-one and genus-three bounding tori.

	System	Parameters	Genus – three	Genus – one
1.	Lorenz	(R, σ, b)	$(28.0, 10.0, 8/3)$	$(278.56, 30.0, 1.0)$
2.	Chen & Ueta	(R, σ, b)	$(22.05, 35.0, 5.0)$	$(35.0, 25.264, 1.0)$
3.	Wang, Singer & Bau			
4.	Shimizu & Morioka	(α, μ)	$(0.375, 0.810)$	$(0.191457, 0.810)$
5.	Rucklidge			
6.	Lusseyran & Brancher			
7.	Burke & Shaw	$(S, \mathcal{V})$	$(0.85, 0.80)$	$(10.0, 4.271)$
8.	Sprott B			
9.	Sprott C			
10.	Rikitake			

(4)

V. PERESTROIKAS OF BOUNDING TORI

A bounding torus of genus three is shown in Fig. 1 [12, 13]. This figure actually shows the projection of the two dimensional surface of the genus-3 torus onto a two-dimensional plane. This projection consists of an outer boundary and three interior holes. The flow directions along all components of this surface are indicated by the arrows. The flows along the outer disk boundary and the two interior holes (shown round) on the left and right are in the same direction. The direction of the flow in the middle interior hole (shown square) changes direction at the four singularities. The direction of the flow at any interior point can be determined by continuity considerations. Since the genus is three, the global Poincaré surface of section is the union of two disjoint disks that are transverse to the flow. The locations of these disks are shown as heavy lines extending between the interior round holes and the exterior boundary in Fig. 1.

Many distinct branched manifolds can exist within the surface of this bounding torus. For any such branched manifold, each branch line can be moved to a disk in the global Poincaré surface of section. All branched manifolds compatible with this bounding torus therefore have two branch lines. One such branched manifold is shown in Fig. 2(a). This branched manifold has six branches, two branch lines, and a two-fold rotation symmetry. The return map for this branched manifold is shown in Fig. 2(b). The two branch lines are labeled L and R. Initial conditions on L are shown along the horizontal segment L and their images under the flow are shown above the initial condition. Initial conditions near the "inside" (see Fig. 2(a)) return to L and those nearer the outside flow to R. The branch labeled 0 connecting L to L has no torsion. The two branches labeled 1 and 2 that connect L to R have torsions of π and 0 radians. This return map shows that tearing occurs between branches 0 and 1, while folding occurs between branches 1 and 2. Initial conditions from branch line R are described in the same fashion [19].

As control parameters change the strange attractor also changes. Small changes include creation and/or annihilation of periodic orbits. Larger changes include inclusion of additional branches or removal of branches already present. For example, the branches 2 ($L \to R$ and $R \to L$) may shrink until the flow no longer goes through them, or these branches may grow until they reach an extremum and turn around, creating new branches ("3"). In all these cases the two branch lines remain present and serve to feed more or fewer branches and the branched manifold remains bounded by a genus-3 bounding torus.

The bounding tori can themselves experience perestroikas. We sketch the general arguments as they apply to a genus-three bounding torus. For simplicity, we assume the flow satisfies a rotation symmetry ($R_Z(\pi)$). However, none of the results described below depends on symmetry. As control parameters change the flow through some of the flow tubes in a bounding torus can be restricted and finally annihilated.

In Fig. 3(a) we show one perestroika that can occur for the genus-3 bounding torus. In this case the flow is restricted in the two interior flow tubes, marked with an $\times$. Flow in these tubes returns from L to L or from R to R. As the flow is restricted, the return map becomes increasingly "offdiagonal," and finally completely offdiagonal, as shown in Fig. 3(b) [19]. In this case all initial conditions on L flow to R and those on R flow to L. This determinism means that one of the two components of the global Poincaré surface of section is redundant. This is consistent with the flow being contained in a genus-one bounding torus. In this case the strange attractor with $4 = 2 \times 2$ branches and 2 branch lines in the genus-3

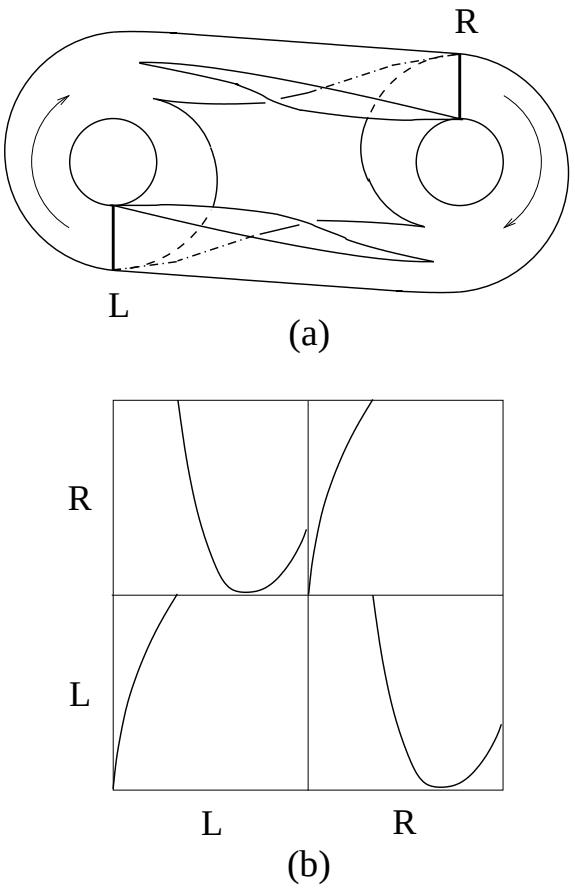

FIG. 2: (a) Branched manifold compatible with the bounding torus shown in Fig. 1. There are two branch lines and six branches. (b) Return map for this branched manifold. Diagonal parts describe the $L \to L$ and $R \to R$ flows and offdiagonal parts describe the $L \to R$ and $R \to L$ flows.

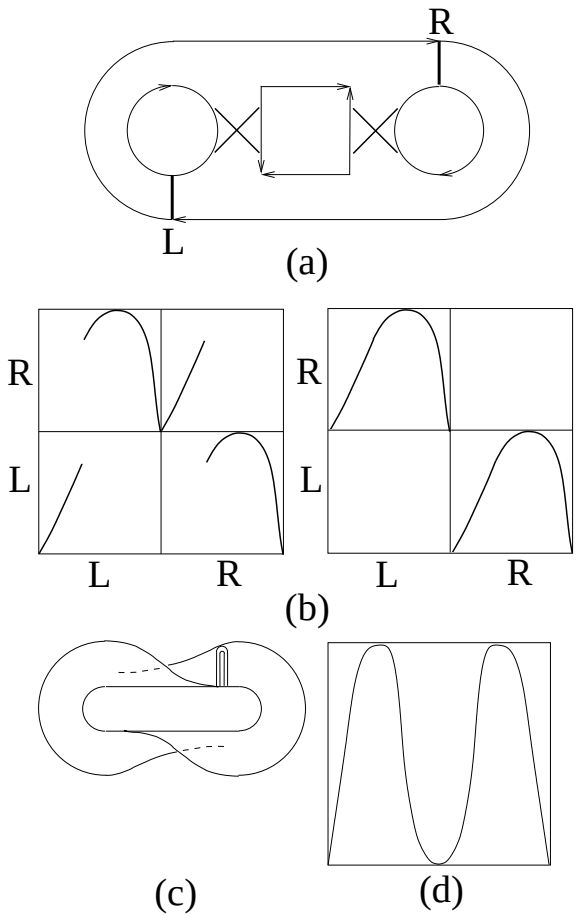

FIG. 3: (a) Flow through the interior flow tubes is restricted. (b) The return map becomes increasingly offdiagonal, finally offdiagonal in the limit that the flow through these two flow tubes is completely restricted. (c) The original strange attractor is deformed into a single strange attractor, with one branch line and $4 = 2^2$ branches, contained within a genus-one bounding torus. (d) The return map on the single branch line has four branches.

bounding torus is deformed and is now embedded in a genus-one bounding torus. The branched manifold has a single branch line and $4 = 2^2$ branches. It is shown in Fig. 3(c). The return map on the single branch line (R) is shown in Fig. 3(d).

In Fig. 4(a) we show what happens when the flow through the two exterior flow tubes marked with an $\times$, that carry the flow from one component of the Poincaré section to the other, is restricted. The return map becomes "more diagonal," and finally diagonal (Fig. 4(b)) when the flow through these two flow tubes is completely cut off. The flow returns from branch line L to branch line L, or from R back to R. The strange attractor is "severed" into two components, each described by a branched manifold with one branch line. Each of these two branched manifolds is enclosed in a genus-one bounding torus. This perestroika generates two genus-1 bounding tori from one genus-3 bounding torus. These are shown in Fig. 4(c). The branched manifolds with each are shown in Fig. 4(d). In this perestroika, a connected genus-3 attractor is transformed to two disjoint genus-1 attractors. The two bounding tori, and any strange attractors in them, are disjoint and unlinked.

VI. MECHANISM CAUSING PERESTROIKAS

Figures 5 and 6 show that the Lorenz attractor undergoes a perestroika as the control parameters change from $(R, \sigma, b) = (28.0, 10.0, 8/3)$ to $(278.56, 30.0, 1.0)$. The perestroika is described by a transition from a genus-3 bounding torus to a genus-one bounding torus. During this change of control parameter values there is no change in the stability properties of the three fixed points but the

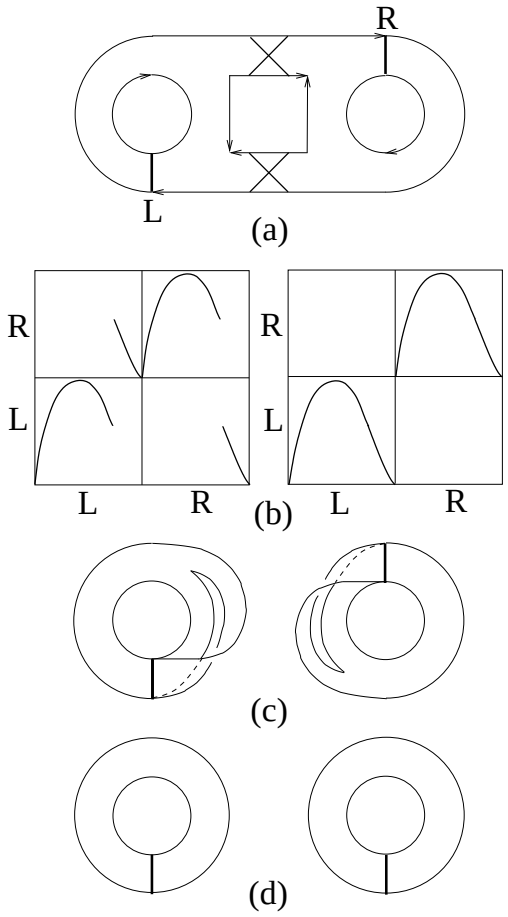

FIG. 4: (a) Flow through the exterior flow tubes is restricted. (b) The return map becomes increasingly diagonal, finally diagonal in the limit that the flow through these two flow tubes is completely restricted. (c) The original strange attractor is deformed into two disjoint strange attractors (d), each in a genus-one bounding torus (c), each with a single branch line.

locations of the two foci change.

The change occurs because changing the control parameter values forces to the flow to visit different neighborhoods of the Z axis. For $(R, \sigma, b) = (28.0, 10.0, 8/3)$ the flow passes near the Z axis for small values of Z ($0 < Z < 30$). In this range of Z values the Z axis has the transverse stability of a saddle. The saddle structrue of the Z axis splits the flow and is responsible for the tearing that is evident in the first return map, shown in Fig. 5(c). For $(R, \sigma, b) = (278.56, 30.0, 1.0)$ the flow passes around the Z axis for much larger values of Z ($275 < Z < 325$). In this range of Z values the transverse stability is that of a focus. The transverse stability of this axis is shown clearly in Fig. 6(a). The projection of the strange attractor onto the X-Y plane (Fig. 6(b)) shows clearly that its bounding torus has genus one, and the first return map [Fig. 6(c)] shows that no tearing occurs.

This mechanism operates to cause a genus-3 to genus-1 perestroika in the other dynamical systems presented in Table 1. The strange attractors of genus-3 type and genus-1 type are shown for the Burke and Shaw dynamical system [35] in Fig. 7, the Chen and Ueta dynamical system [30] in Fig. 8, and the Shimizu-Morioka dynamical system [32] in Fig. 9.

Figure 10 provides a schematic representation of this mechanism. When the control parameter values cause the flow to pass the Z axis in a neighborhood where it has the transverse stability of a focus, only folding occurs and the attractor can be enclosed in a genus-one torus. When the flow passes the Z axis in a neighborhood where it has the transverse stability of a saddle, tearing occurs and the attractor can be enclosed in a genus-3 torus. In the transition region both folding and tearing occur, as illustrated in the middle of Fig. 10. As long as tearing occurs, the attractor is enclosed in a genus-3 surface. We point out that the perestroika is not driven by change of stability of the fixed point on the Z axis (when there is one), or even the existence of a fixed point on the Z axis (cf. Table 1, systems 7-10), only by the transverse stability properties of the Z axis where the flow approaches it. The mechanism shown in Fig. 10 is responsible for creating the genus-3 to genus-1 perestroikas of the type shown in Fig. 3, where flow through the two interior flow tubes is restricted and finally annihilated.

VII. OTHER MECHANISMS

Mechanisms for creating perestroikas of the type shown in Fig. 4 have also been observed. In these mechanisms flow through the exterior flow tubes is restricted and finally annihilated. The result is a pair of symmetry-related strange attractors, each of genus-one type. Fig. 11 shows this transition for the Lorenz system. In effect, changing the control parameter values reduces and finally annihilates the flow past the Z axis. The two strange attractors that result are unlinked.

Another mechanism can create a pair of symmetry-related strange attractors that are linked. The mechanism that generates this perestroika can be considered in two steps. First, the control parameters are changed from $(R, \sigma, b) = (28.0, 10.0, 8/3)$ to values for which a genus-one strange attractor exists. The attractor at $(R, \sigma, b) = (142.5, 10.0, 8/3)$ is shown in Fig. 12(a). Its return map on a global Poincaré surface of section is shown in Fig. 12(b). The attractor has ? branches and a global torsion of ?. The global torsion is determined by the self relative rotation rates of the unstable periodic orbits in the attractor. It can also be identified by carrying out the isotopic deformation shown in Fig. 12(c). This smooth transformation converts writhe to twist, or torsion.

A mechanism leading to a new perestroika is illustrated

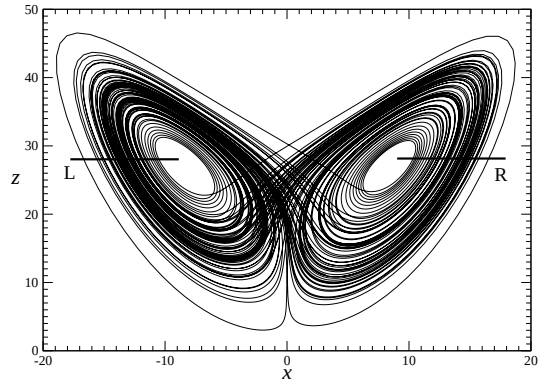

(a) X-Z plane projection

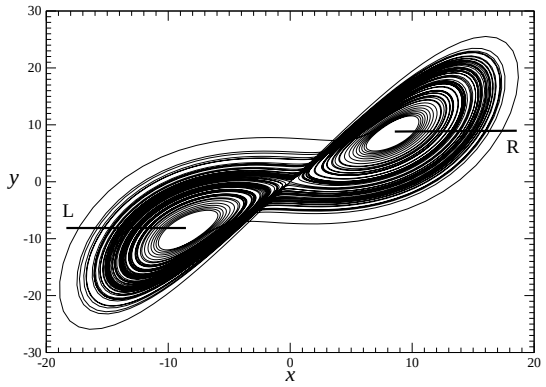

(b) X-Y plane projection

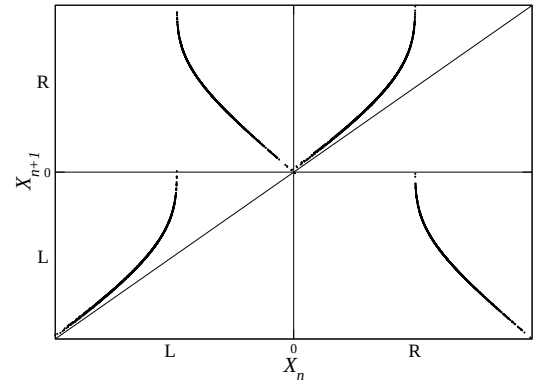

(c) First return map

FIG. 5: Projection of the Lorenz attractor onto (a) the X-Z plane and (b) the X-Y plane. The two components of the global Poincaré section are shown. (c) Return map on the two branch lines shows that tearing occurs. Parameter values: $(R, \sigma, b) = (28.0, 10.0, 8/3)$.

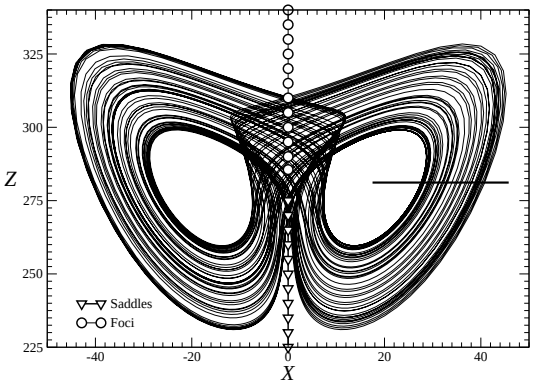

(a) X-Z plane projection

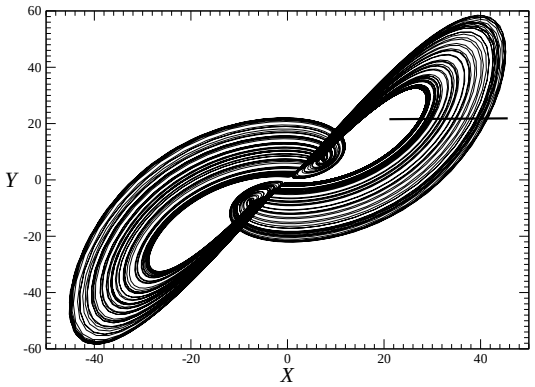

(b) X-Y plane projection

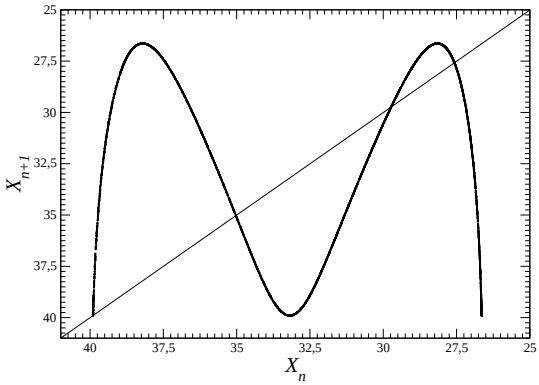

(c) First-return map

FIG. 6: Projection of the Lorenz attractor onto (a) the X-Z plane and (b) the X-Y plane. (c) First-return map to a single component Poincaré section shows that only folding occurs. Parameter values: $(R, \sigma, b) = (278.56, 30.0, 1.0)$.

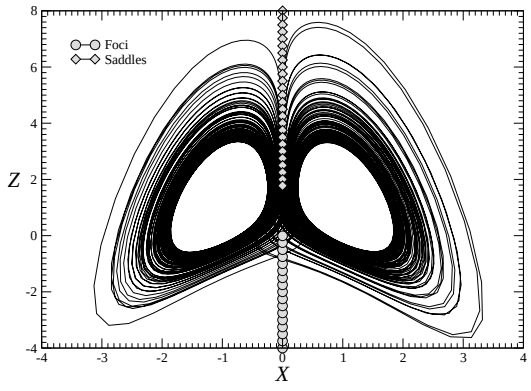

(a) Tearing: $(S, \mathcal{V}) = (0.85, 0.80)$

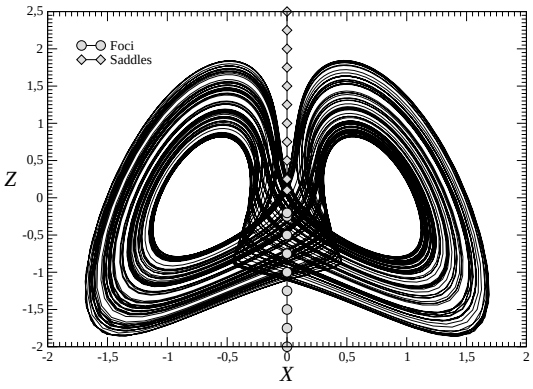

(b) Folding:$(S, \mathcal{V}) = (10, 4.271)$

FIG. 7: Chaotic attractors for the Burke and Shaw system. (a) Attractor with a tearing mechanism occurs around the upper part of the Z-axis which has the transverse stability of saddles. (b) Attractor with a folding mechanism occurs around the lower part of the Z-axis which has the transverse stability of foci.

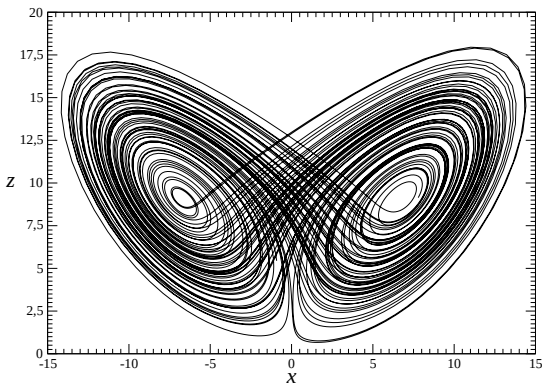

(a) Tearing:$(R, \sigma, b) = (22.05, 35, 5)$

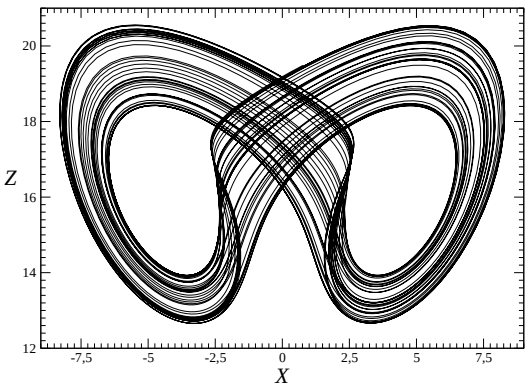

(b) Folding: $(R, \sigma, b) = (35, 25.264, 1)$

FIG. 8: Chaotic attractors for the Chen and Ueta system. (a) Attractor with a tearing mechanism contained in a bounding torus of genus-three and (b) attractor with a folding mechanism contained in a bounding torus of genus one.

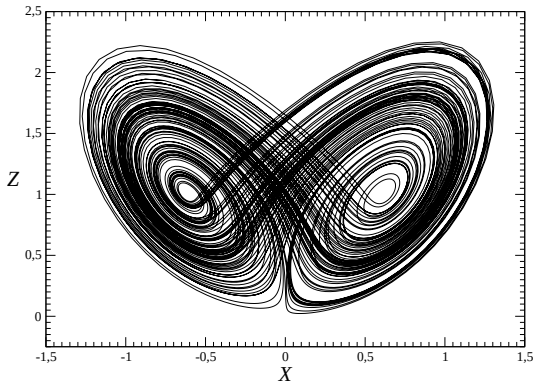

(a) Tearing: $\alpha = 0.375$

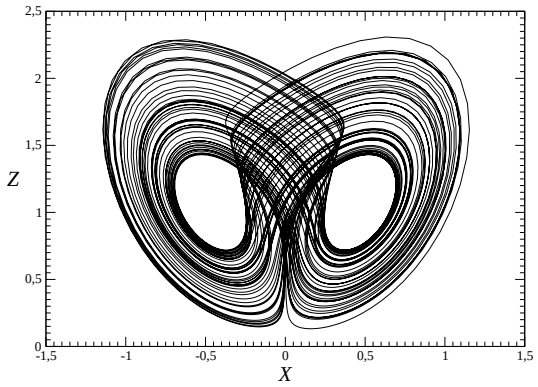

(b) Folding: $\alpha = 0.191457$

FIG. 9: Chaotic attractors for the Shimizu and Morioka system with $\mu = 0.810$. (a) Tearing mechanism within a torus of genus-three and (b) folding mechanism within a genus-one torus.

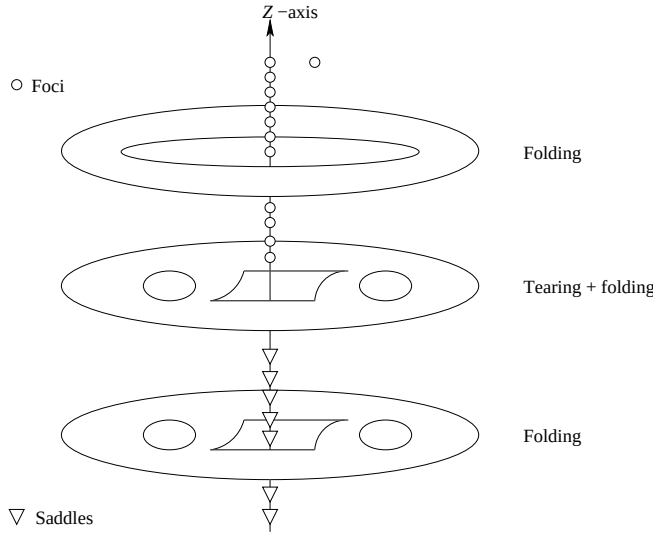

FIG. 10: As control parameters vary the attractor flows past the Z axis in different regions. Folding occurs when the transverse stability is that of a focus and tearing occurs when the trasnverse stability is that of a saddle. Both occur in the transition region.

FIG. 11: Lorenz perestroika shows a genus-3 to 2 × genus-1 transition. (a) genus-3 (b) unlinked symmetry-related genus-one strange attractors.

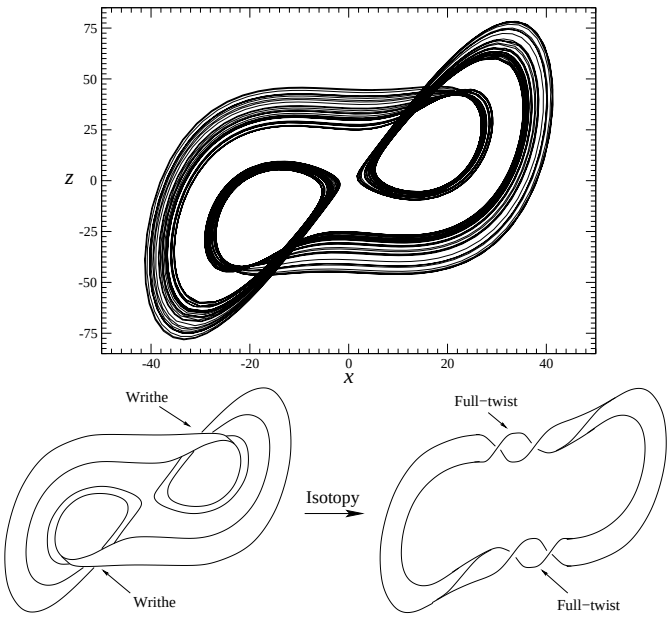

FIG. 12: (a) Lorenz attractor after the saddle fails to split the flow, deflecting it to a single region in the state space. The attractor can be bounded by a genus-one torus, so only one branch line is necessary. (b) Return map on the branch line. (c) The local torsion can be determined by an isotopy that exchanges writhe for twist. Parameter values: $(R, \sigma, b) = (142.5, 10, 8/3)$.

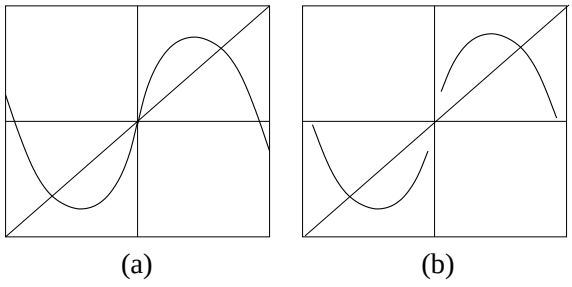

FIG. 13: Return maps for (a) connected strange attractor and (b) two disconnected strange attractors that are linked with linking number n.

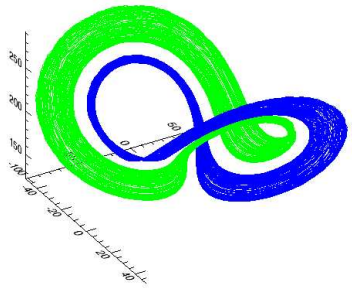

FIG. 14: (a) Two linked genus-one strange attractor generated by the Lorenz equations and (b) their return map. Parameter values $(R, \sigma, b) = (?, ?, ?)$.

in Fig. 13 in terms of return maps. Fig. 13(a) shows a return map for a strange attractor that can be enclosed in a genus-one bounding torus. In this return map the internal branch with positive slope has an even local torsion, $2n$. The two outer branches with negative slope have local torsion $2n \pm 1$. If the control parameters are varied to generate the return map shown in Fig. 13(b), the attractor becomes disconnected. The two disconnected pieces have linking number n and are unlinked if $n = 0$. Two linked attractors satisfying the Lorenz equations are shown in Fig. 14(a). The return maps in an appropriate half-plane are shown in Fig. 14(b).

VIII. SUMMARY AND CONCLUSIONS

As experimental conditions or control parameters change, strange attractors also change. The changes can be described by a hierarchy with three levels of structure. At the first level is the set of unstable periodic orbits in the attractor. At the next level of structure are the branched manifolds that describe the unstable periodic orbits in the strange attractor. Branched manifolds can metamorphize by the addition of new branches or the deletion of old branches as control parameters vary. At the grossest level in this heirarchy, the bounding tori that enclose the branched manifolds can change. In this work we have described some changes that can occur and exhibited mechanisms responsible for bounding tori perestroikas in a large class of simple dynamical systems. This special class exhibits a rotation symmetry $[R_Z(\pi)]$, but the mechanism operates when the symmetry is broken or absent.

In general, the mechanism involves restricting the flow through either interior (Fig. 3) or exterior (Fig. 4) flow tubes of a bounding torus, with the following consequences:

Restriction	Initial	Final
Interior flow tube	genus-3 $\rightarrow$	genus-1
Exterior flow tube	genus-3 $\rightarrow$ 2 $\times$	genus-1

The two genus-one bounding tori, and the strange attractors enclosed by them, are not linked.

We exhibited another mechanism in which a strange attractor enclosed in a genus-one bounding torus bifurcates to a pair of strange attractors. Each is enclosed in a genus-one bounding torus, and the two tori are linked with nonzero linking number n. The Lorenz equations exhibit a perestroika of this type. It can be summarized as

genus-3 $\rightarrow$ genus-1 $\rightarrow$ 2 $\times$ genus-1 (linked)

It may seem that such a bifurcation cannot occur directly from a genus-3 strange attractor, and that it must proceed through the genus-one stage. This is not necessarily so. If the genus-3 bounding torus, for which the intrinsic (as seen from "inside") representation is as shown in Fig. 1, is actually embedded in R^3 as shown in Fig. 15, then restricting the flow in the external flow tubes can produce the perestroika

genus-3 $\rightarrow$ 2 $\times$ genus-1 (linked)

in a single step.

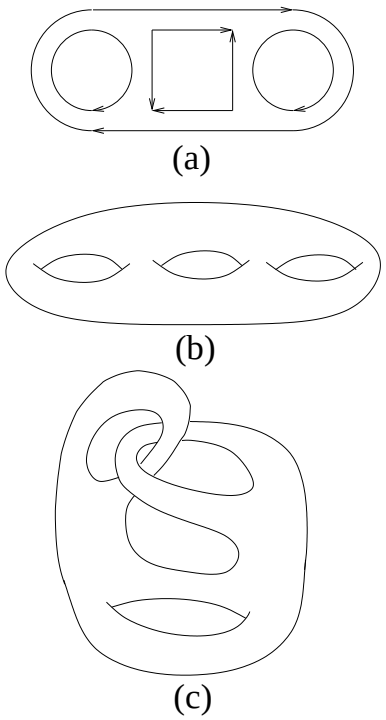

FIG. 15: (a) Canonical form for a genus-three bounding torus describes only intrinsic properties (how it looks from the inside). The extrinsic properties are governed by how the torus is embedded in R^3. Extrinsic embedding that is (b) unknotted and (c) knotted so that when the flow through the external flow tubes is restricted two linked genus one attractors are formed.

This work was partly done during a stay by C.L. at Drexel University. This work was supported in part by NSF Grant PHY9987468.

REFERENCES

[1] N. B. Tufillaro, T. Abbott, and J. Reilly, *An Experimental Approach to Nonlinear Dynamics and Chaos*, (Addison-Wesley, Reading, MA, 1992).

[2] E. Ott, *Chaos in Dynamical Systems*, (Cambridge University Press, Cambridge, 1993).

[3] H. G. Solari, M. A. Natiello, and G. B. Mindlin, *Nonlinear Dynamics: A Two-Way Trip from Physics to Math*, (IOP Publishers, London, 1996).

[4] R. Gilmore, Topological analysis of chaotic dynamical systems, *Reviews of Modern Physics* **70**(3), 1455-1530 (1998).

[5] R. Gilmore and M. Lefranc, *The Topology of Chaos*, (Wiley, NY, 2002).

[6] V. I. Arnol'd, S. M. Gusein-Zade, and A. N. Varchenko, *Singularities of Differentiable Mappings I.* (Birkhäuser, 1985).

[7] R. Gilmore, *Catastrophe Theory for Scientists and Engineers*, (Wiley, NY, 1981).

[8] V. I. Arnol'd, *Catastrophe Theory* (2nd Ed.), (Springer-Verlag, NY, 1986).

[9] T. Poston and I. N. Stewart, *Catastrophe Theory and its Applications*, (Pitman, London, 1978).

[10] J. Birman and R. F. Williams, Knotted periodic orbits in dynamical systems I: Lorenz's equations, *Topology* **22**, 47-82 (1983).

[11] J. Birman and R. F. Williams, Knotted periodic orbits in dynamical systems II: Knot holders for fibered knots, *Cont. Math.* **20**, 1-60 (1983).

[12] T. D. Tsankov & R. Gilmore, Strange attractors are classified by bounding tori, *Physical Review Letters*, **91** (13), 134104 1-4, 2003.

[13] T. D. Tsankov & R. Gilmore, Topological aspects of the structure of chaotic attractors in $\mathbb{R}^3$, *Physical Review E*, **69**, 056206 1-11 (2004).

[14] N. B. Tufillaro, H. G. Solari, and R. Gilmore, Relative rotation rates: fingerprints of strange attractors, *Phys. Rev. A***41**, 5717-5720, (1990)

[15] G. B. Mindlin, X.-J. Hou, H. G. Solari, R. Gilmore, and N. B. Tufillaro, Classification of strange attractors by integers, *Phys. Rev. Lett.* **64**, 2350-2353 (1990).

[16] G. B. Mindlin, H. G. Solari, M. A. Natiello, R. Gilmore, and X.-J. Hou, Topological analysis of chaotic time series from the Belousov-Zhabotinskii reaction, *Journal of Nonlinear Science* **1**, 147-173 (1991).

[17] J. Katriel and R. Gilmore, Entropy of bounding tori (unpublished).

[18] T. D. Tsankov, A. Nishtala and R. Gilmore, Embeddings of a strange attractor into R^3, *Phys. Rev. E***69**, 056215 1-8 (2004).

[19] G. Byrne, R. Gilmore & C. Letellier, Distinguishing between folding and tearing mechanisms in strange attractors, *Phys. Rev. E*(in press)

[20] O. E. Rössler, An equation for continuous chaos, *Phys. Lett. A***57**, 397-398 (1976).

[21] G. B. Mindlin, R. Lopez-Ruiz, H. G. Solari, and R. Gilmore, Horseshoe implications, *Phys. Rev. E***48**(6), 4297-4304 (1993).

[22] T. Hall, Weak universality in two-dimensional transitions to chaos, *Phys. Rev. Lett. 71*(1), 58-61 (1993).

[23] T. Hall, The creation of horseshoes, *Nonlinearity***7**, 861-924 (1994).

[24] M. A. Natiello and H. G. Solari, Remarks on braid theory and the characterization of periodic orbits, *J. Knot Theory Ramifications***3**, 511-529 (1994).

[25] R. Gilmore and X. Pei, The topology and organization of unstable periodic orbits in Hodgkin-Huxley models of receptors with subthreshold oscillations, *Handbook of Biological Physics, Vol. 4, Neuro-informatics, Neural Modeling*, (F. Moss and S. Gielen, Eds.), Amsterdam, North Holland, 2001, pp. 155-203.

[26] R. Miranda and E. Stone, The proto-Lorenz system, *Phys. Lett. A***178**, 105-113 (1993).

[27] C. Letellier and R. Gilmore, Covering dynamical systems : Two-fold covers, *Physical Review E***63**, 016206, (2001).

[28] D. A. Cox, J. B. Little, and D. O'Shea, *Ideals, Varieties, and Algorithms*, (Springer-Verlag, NY, 1996).

[29] E. N. Lorenz. Deterministic nonperiodic flow. *Journal of the Atmospheric Sciences,* **20**, 130-141, 1963.

[30] G. Chen & T. Ueta, Yet another chaotic attractor, *International Journal of Bifurcation and Chaos*, **9**, 1465-1466, 1999.

[31] Y. Wang, J. Singer & H. H. Bau, Controlling chaos in a thermal convection loop, *Journal of Fluid Mechanics*, **237**, 479-498, 1992.

[32] T. Shimizu & N. Morioka. On the bifurcation of a symmetric limit cycle to an asymmetric one in a simple model, *Physics Letters A*, **76**, 201-204, 1980.

[33] A. M. Rucklidge, Chaos in models of double convection, *Journal of Fluid Mechanics*, **237**, 209-229, 1992.

[34] F. Lusseyran & J. P. Brancher. Some results on simple dynamo systems, *IEEE Transactions on Magnetics*, **26** (5), 2875-2879, 1990.

[35] R. Shaw. Strange Attractor, Chaotic Behavior and Information Flow, *Zeitschrift für Naturforschung A*, **36**, 80-112, 1981

[36] J. S. Sprott. Some simple chaotic flows, *Physical Review E*, **50** (2), 647-650, 1994.

[37] T. Rikitake, Oscillations of a system of disk dynamos, *Proceedings of the Cambridge Philosophical Society*, **54**, 89-105, 1958